Accepted Manuscript

Design, synthesis and biological evaluation of 4-anilinoquinoline derivatives as novel potent tubulin depolymerization agents

Yuanyuan Zhou, Wei Yan, Dong Cao, Mingfeng Shao, Dan Li, Fang Wang, Zhuang Yang, Yong Chen, Linhong He, Taijin Wang, Mingsheng Shen, Lijuan Chen

PII: S0223-5234(17)30562-7

DOI: 10.1016/j.ejmech.2017.07.040

Reference: EJMECH 9603

To appear in: *European Journal of Medicinal Chemistry*

Received Date: 23 March 2017

Revised Date: 19 May 2017

Accepted Date: 20 July 2017

Please cite this article as: Y. Zhou, W. Yan, D. Cao, M. Shao, D. Li, F. Wang, Z. Yang, Y. Chen, L. He, T. Wang, M. Shen, L. Chen, Design, synthesis and biological evaluation of 4-anilinoquinoline derivatives as novel potent tubulin depolymerization agents, *European Journal of Medicinal Chemistry* (2017), doi: 10.1016/j.ejmech.2017.07.040.

Graphical abstract

Design, synthesis and biological evaluation of 4-anilinoquinoline derivatives as novel potent tubulin depolymerization agents

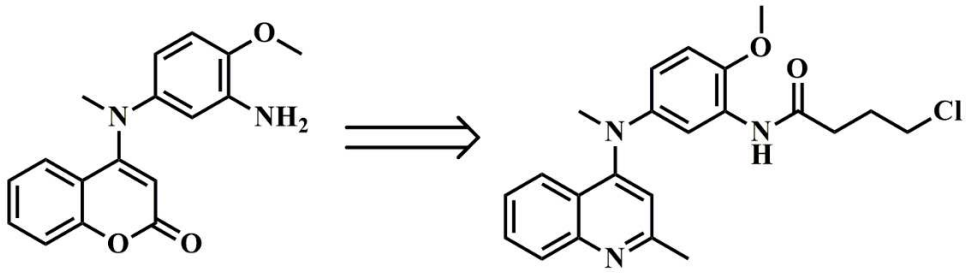

IC_{50} = 10 nM IC_{50} = 1.5 nM

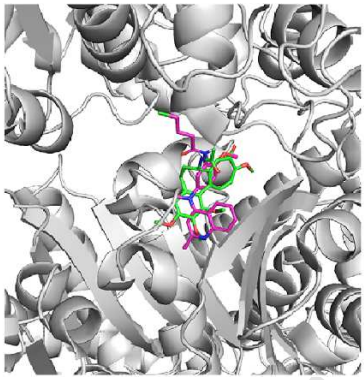

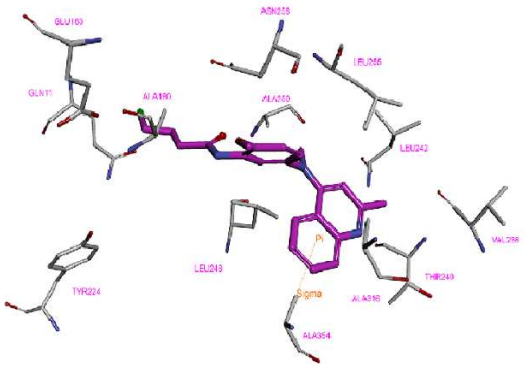

Design, synthesis and biological evaluation of 4-anilinoquinoline derivatives as novel potent tubulin depolymerization agents

Yuanyuan Zhou[a,1], Wei Yan[a,1], Dong Cao[b], Mingfeng Shao[a], Dan Li[a], Fang Wang[a], Zhuang Yang[a], Yong Chen[a], Linhong He[a], Taijin Wang[a], Mingsheng Shen[a], Lijuan Chen[a,c,*]

[a.] State Key Laboratory of Biotherapy and Cancer Center, West China Hospital, Sichuan University and Collaborative Innovation Center, Chengdu, 610041, China

[b.] Chengdu Institute of Chinese Herbal Medicine, Chengdu, 610043, China

[c.] School of Chemical Engineering, Sichuan University, Chengdu, China

ABSTRACT:

A series of novel 4-anilinoquinoline derivatives were synthesized and evaluated for their antiproliferative activities. Among them, **14h** exhibited the most potent cytotoxic activity with IC_{50} values ranging from 1.5 to 3.9 nM against all tested cancer cell lines, and showed promising efficacy in multidrug resistant cancer cells. Flow cytometry assay, immune-fluorescence staining, microtubule dynamics assays and competition assays with EBI identified that **14h** was a novel tubulin depolymerization agent by binding to the colchicine site. Importantly, in vivo efficacy evaluation of HCT116 xenograft model, **14h** showed efficient antitumor activity without significant loss in body weight. All the results indicated that **14h** could be a promising candidate for the treatment of cancer.

Keywords: quinoline, antiproliferative, microtubules, depolymerization, antimitotic.

1. Introduction

Microtubules, mainly composed of α/β-tubulin heterodimers [1], are the basic constituents of eukaryotic cell and play a crucial role in many fundamental cellular processes such as cell division, formation, regulation of motility, cell signaling, secretion, maintenance of cell shape, and intracellular transport [2-4]. Consequently, the microtubule has become an attractive target for the design and development of novel antimitotic agents for cancer therapy [5-7]. Antimitotic agents are generally classified into two major categories: microtubule stabilizing agents (e.g., paclitaxel) and polymerization inhibitors (e.g., colchicine) [8, 9]. Antitumor drugs targeting microtubules can directly affect cell mitosis, and lead to cell division stagnated in G2/M phase [6, 7].

These antimitotic agents were found targeting several different binding sites, including the taxane site, the vinca site, the colchicine site, and so on [10-12]. In contrast to develop the taxane or vinca alkaloid binding sites, more attention has been drawn to the inhibitors which target to colchicine sites, due to its potential of overcoming the ABC-transporter-mediated drug resistance [13-15]. Currently, several colchicine site inhibitors have been reported, such as colchicine (**1**), combretastatin A-4 (CA-4, **2**), etc. CA-4 was first isolated from the African bush willow *Combretum caffrum*, and exhibited potent antitumor activity against several cancer cells [16, 17]. CA4P (**3**), a water-soluble phosphate prodrug of CA-4, has been approved by both the FDA and EMA for using in anaplastic thyroid cancer [17, 18]. Previously, a 4-anilinocoumarin derivative (**4**) was synthesized by our group and showed potent

antiproliferative activity against all tested cancer cell lines. It had IC_{50} values ranging from 3.3 to 23.4 nM. Compound **4** was also reported as microtubule agents by binding to the colchicine site [19]. In the present study, a series of new quinoline derivatives have been designed and synthesized as tubulin inhibitors, as an attempt to investigate whether the coumarin ring could be replaced with the quinoline one.

Quinoline-based derivatives, an important class of heterocyclic compounds, exhibit anticancer activity with different mechanisms including alkylating agents [20], tyrosine kinase inhibitors [21, 22] and tubulin inhibitors [23, 24]. Molecular docking analysis [25] (**Figures S1 in Supporting Information**) proved that it was feasible to replace the coumarin ring of **4** with the quinoline ring, and compound **13b** was designed. According to the docking results, and it can be speculated that **13b** is a novel tubulin agent targeting colchicine sites. Based on the structural modification and optimization of compound **13b**, diverse derivatives (**14a-m** and **15a-e**) were synthesized and evaluated for their antiproliferative abilities. (**Figure 1**)

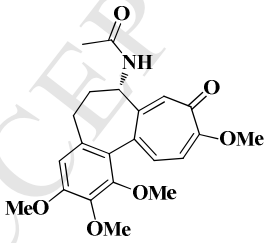

Colchicine (1)

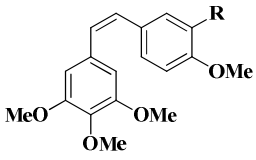

CA-4 (2, R=OH)
CA4P (3, R=OPO_3Na_2)

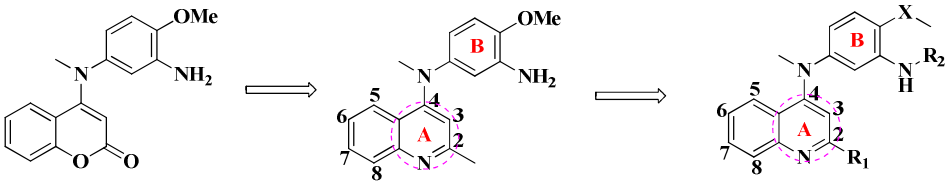

4 13b 9a-d, 13a-d 14a-m, 15a-e

Figure 1. Some reported tubulin depolymerization agents. 4-anilinoquinoline general structure **13b** is derived from a combination of 4-anilinocoumarin (**4**).

2. Results and discussion

2.1. Chemistry

4-Substituted quinoline derivatives (**9a-d**) were first prepared by the synthesis method outlined in **Scheme 1**. **5a-c** in phosphorus oxychloride refluxed for 12 h to give **6a-c**. **6a-c** and **7a** in isopropanol with catalytic amount of HCl (conc.) refluxed for 2 h to give **8a-c**. **6b** reacted with **7b** to give **8d** by following the same route. Compounds **8a-d** reacted with sodium hydride and iodomethane to obtain **9a-d**, respectively.

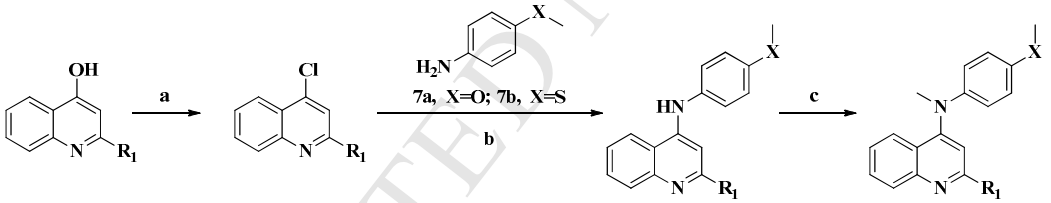

5a, R_1=Cl
5b, R_1=Me
5c, R_1=H

6a, R_1=Cl
6b, R_1=Me
6c, R_1=H

8a, R_1=Cl, X=O
8b, R_1=Me, X=O
8c, R_1=H, X=O
8d, R_1=Me, X=S

9a, R_1=Cl, X=O
9b, R_1=Me, X=O
9c, R_1=H, X=O
9d, R_1=Me, X=S

Scheme 1. Reagents and conditions: (a) $POCl_3$, 80 °C, 4 h. (b) HCl (conc.), $(Me)_2CHOH$, 80 °C, 2 h. (c) NaH, CH_3I, DMF, 0 °C, 1h, rt, 1 h.

Compounds **13a-d** and **14a-m** were synthesized by the synthesis route shown in **Scheme 2**. **6a-c** and **10a** with catalytic amount of HCl (conc.) refluxed in isopropanol for 2 h to give **11a-c**. **6b** reacted with **10b** to give **11d** following the similar approach. **11a-d** were treated with sodium hydride and iodomethane to give **12a-d**, respectively. Compounds **12a-d** in ethanol and water were added iron powder and ammonium

chloride to obtain **13a-d**, respectively**.** Then we used the appropriate various acyl chlorides to react with **13b** to obtain **14a-m**, respectively. As shown in **Scheme 3**, compounds **15a-e** were easily prepared from **14f** react with different amines.

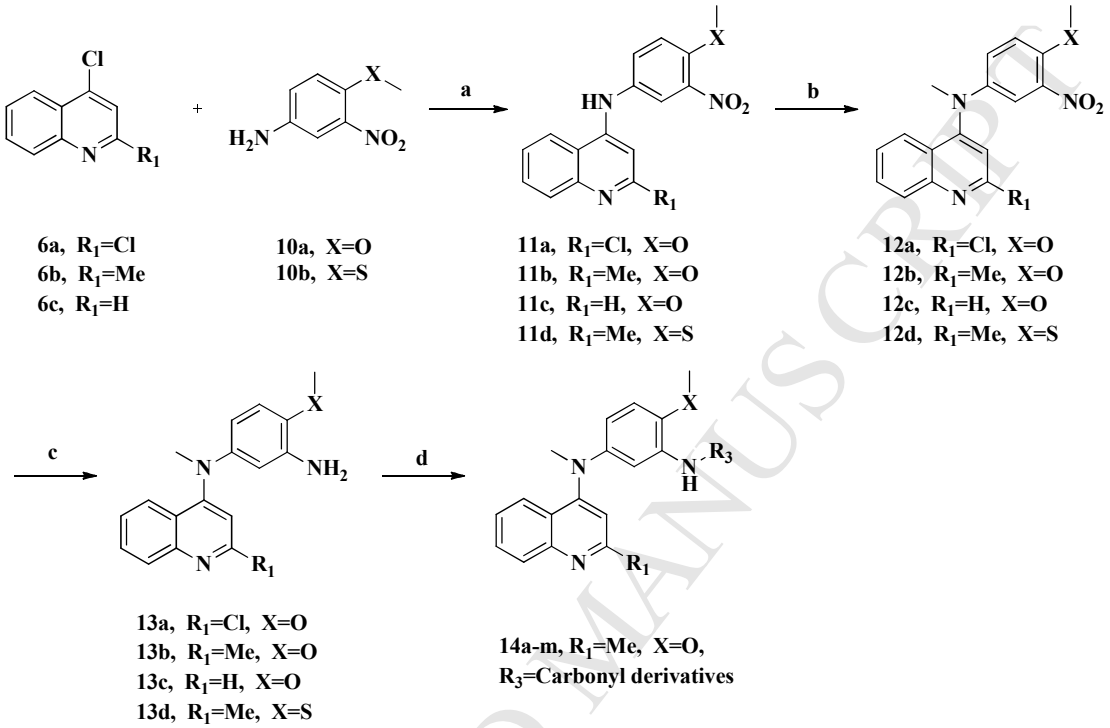

Scheme 2. Reagents and conditions: (a) HCl (conc.), $(Me)_2CHOH$, 80 °C, 2 h. (b) NaH, CH_3I, DMF, 0 °C, 1 h, rt 1 h. (c) Fe powder, NH_4Cl, CH_3CH_2OH/H_2O (3:1, v/v), 80 °C. (d) RCO_2Cl, Et_3N, CH_2Cl_2, rt, 0.5 h.

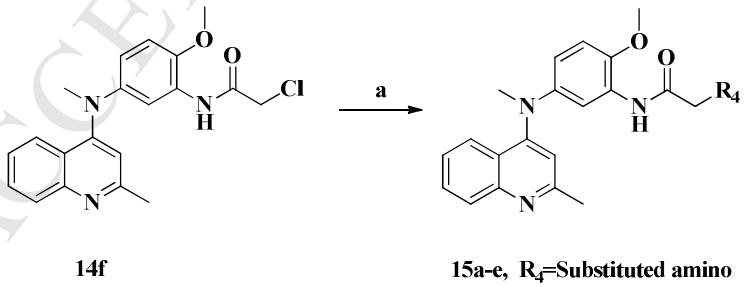

Scheme 3. Reagents and conditions: (a) R'NH R, K_2CO_3, CH_3CN, 80 °C, 2 h.

2.2. Biological evaluation

2.2.1. In vitro antiproliferative activities.

The synthesized derivatives **9a-d** and **13a-d** were evaluated for antiproliferative activities against MDA-MB-231 cells (human breast cancer cells) using MTT assay and colchicine was included as the reference compound [26]. The results were summarized in **Table 1**. Compound **9b** (containing methyl in the 2-position of the A-ring) displayed potent inhibitory activity with an IC_{50} value of 6.6 nM. In contrast, both the 2-Cl analog (**9a**) and 2-H analog (**9c**) showed poor inhibitory activities (IC_{50} > 500 nM). The similar outcomes can be found in the comparison of **13a** and **13C** with **13b**. It can be concluded that the methyl in the 2-position of the A-ring is necessary to maintain the inhibitory activity of the series of compounds. It has been reported that the in vitro phase I biotransformation of CA-4 in hepatic microsomal involves O-demethylation [27]. The compounds of the 4-methylthio substituent group in the B-ring were synthesized to block O-demethylation metabolic pathway. Compounds **9d** and **13d** (IC_{50}, 15.5 and 9.5 nM, respectively) presented a slightly decreased inhibition activities compared to **9b** and **13b** (IC_{50}, 6.6 and 3.2 nM, respectively**)** when methylthio was introduced to the para-position of benzene. It should be noted that both **13b** and **13d** with amino group exhibited stronger inhibitory activities compared to the corresponding compounds **9b** and **9d**. It can be concluded that the amino was an important group to maintain the antiproliferative activity. Among the above compounds, **13b** (containing methyl in the 2-position of the A-ring, amino in the 3-position and methoxy group in the 4-position of the B-ring) exhibited the optimal antiproliferative activity.

Table 1. The in vitro antiproliferative activities of **9a-d** and **13a-d** against MDA-MB-231 cells

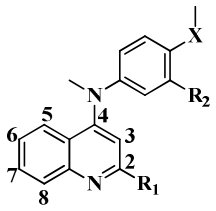

Compd	X	R_1	R_2	IC_{50}[a], nM
9a	O	Cl	H	>500
9b	O	Me	H	6.6 ± 0.7
9c	O	H	H	>500
9d	S	Me	H	15.5 ± 0.2
13a	O	Cl	NH_2	43.1 ± 0.6
13b	O	Me	NH_2	3.2 ± 0.8
13c	O	H	NH_2	>500
13d	S	Me	NH_2	9.5 ± 0.4
colchicine				38.2 ± 1.8

[a] 50% inhibitory concentration after drug treatment. Data are expressed as the mean ± SD from the dose-response curves of at least three independent experiments.

Although **13b** showed the best antiproliferative activity against MDA-MB-231 cells, the compound still suffered from poor water solubility. In order to improve the solubility of **13b**, we subsequently modified the 3-amino group on B-ring with aliphatic chain to obtain diverse derivatives **14a-m** and **15a-e**. As expected in **Table 2**, compounds containing different aliphatic chain alkanes, **14a-d**, caused gradient decrease of inhibitory activities with the increase of the length of the alkyl chain, with IC_{50} values ranging from 9.1 to 82.4 nM. There was a slight decrease in inhibitory activity compared to **13b** when propylene bond was introduced to the amide to obtain

14e, with an IC_{50} value of 43.4 nM. The results indicated that introduction of the unsaturated bond decreased the antiproliferative activity. According to our previous experience [19], chlorinated alkanes with different chain length were also introduced to furnish derivatives **14f-i**. As expected, the antiproliferative activities of these compounds decreased with the increase of the length of the alkyl chain. Surprisingly, **14h** with three carbon chlorinated alkane did not fit into the pattern. **14h** showed potent antiproliferative activity with an IC_{50} value of 3.9 nM against MDA-MB-231 cell. The specific mechanism is still unclear. The chlorine of **14f** was replaced with bromine to obtain compound **14j** (IC_{50}, 87.2 nM) resulting in decreased activity. The results indicated that the chlorine product was more potent than bromine derivative. Introduction of ester bonds to obtain **14k-m** caused a great decrease of antiproliferative activities compared to **13b**. Then the chlorine of **14f** was replaced with a series of different amines to explore more effective compounds (**15a-e**), but the tactics resulted in decreased activity (**Table 3**). The results suggested that chlorine product was more potent than ester bonds or amines derivatives.

Table 2. The in vitro antiproliferative activities of **14a-m** against MDA-MB-231 cells

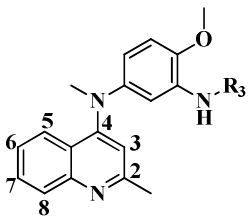

Compd	R_3	IC_{50}[a], nM	Compd	R_3	IC_{50}[a], nM
14a		9.1 ± 0.2	**14h**	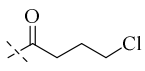	3.9 ± 0.1

14b	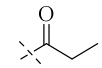	18.5 ± 1.5	**14i**	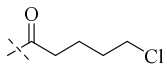	363.3 ± 67.8
14c	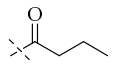	58.4 ± 1.7	**14j**		87.2 ± 14.3
14d	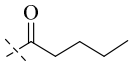	82.4 ± 6.3	**14k**		>500
14e		43.4 ± 9.9	**14l**	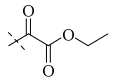	442.6 ± 32.8
14f		6.6 ± 3.9	**14m**	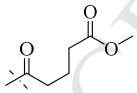	185.5 ± 69.8
14g	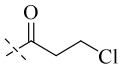	96.6 ± 0.7	**colchicine**		38.2 ± 1.8

[a] 50% inhibitory concentration after drug treatment. Data are expressed as the mean ± SD from the dose-response curves of at least three independent experiments.

Table 3. The in vitro antiproliferative activities of **15a-e** against MDA-MB-231 cells

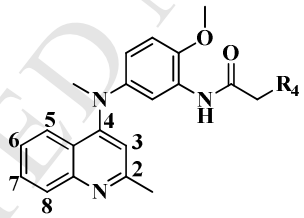

Compd	R_4	IC_{50}[a], nM
15a	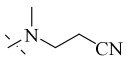	>500
15b	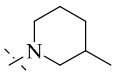	394.0 ± 46.2
15c		256.0 ± 7.5
15d		>500
15e	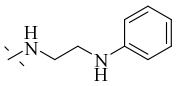	83.6 ± 4.5
colchicine		38.2 ± 1.8

[a] 50% inhibitory concentration after drug treatment. Data are expressed as the mean ± SD from the dose-response curves of at least three independent experiments.

Although several compounds displayed potent antitumor activity with low nanmolar IC_{50} values, these compounds were also subject to the challenge of poor water solubility. It is a major obstacle for further testing in vivo. According to the solubility detecting results (**Table S1 in Supporting Information**), compound **14h** was identified for further biological activity evaluation.

The antiproliferative activity of **14h** on normal human cell lines and various human tumor cell lines was investigated, with colchicine as the positive control. These tumor cells were derived from human colon, lung, ovarian and breast cancers (**Table 4**). **14h** possessed potent inhibitory activity with IC_{50} values ranging from 1.5 to 75.6 nM. It is worth noting that **14h** is more potent than colchicine against all the tested tumor cell lines.

Table 4. Activity of compound **14h** and colchicine against various human tumor cell lines and non-tumoral cell lines

tumor type	cell line	IC_{50}[a], nM	
		14h	**colchicine**
colon	HCT-8	3.4 ± 0.2	13.4 ± 0.1
	HCT116	2.7 ± 0.2	13.9 ± 1.5
lung	A549	3.2 ± 0.3	32.7 ± 0.1
ovarian	A2780S	2.2 ± 0.2	12.3 ± 0.6
breast	MCF-7	1.5 ± 0.1	13.4 ± 0.8
	MDA-MB-231	3.9 ± 0.1	38.2 ± 1.8
normal	LO2	75.6 ± 0.9	26.5 ± 0.7
	HEK-293	45.3 ± 0.8	10.2 ± 0.9

[a] 50% inhibitory concentration after drug treatment. Data are expressed as the mean ± SD from the dose-response curves of at least three independent experiments.

2.2.2. Effect on multidrug resistant cells

Drug resistance is a major obstacle for the first-line chemotherapy [13, 28]. The common mechanism of resistance identified in preclinical or clinical study involves two main categories: the overexpression of a cellular membrane protein called P-glycoprotein (P-gp) and changing in the levels of expression of different β-tubulin isotypes (β-III gene) [29-33]. As it has been known, paclitaxel resistant HCT-8/T (human colon cancer cell line), vinblastine resistant HCT-8/V (human colon cancer lines), and adriamycin resistant MCF-7/ADR (human breast cancer cell line) are all P-gp overexpressed, and paclitaxel resistant A2780/T (human ovarian cancer cell lines) are β-tubulin III overexpressed [34-37]. Hence, the activity of **14h** in these resistant and their related sensitive cancer cells was compared, with paclitaxel, vinblastine and adriamycin as reference compounds. As shown in **Table 5**, **14h** exhibited potent cytotoxic activity against A2780/T (IC_{50} of 3.7 nM), HCT-8/T (IC_{50} of 3.5 nM), HCT-8/V (IC_{50} of 3.5 nM), and MCF-7/ADR (IC_{50} of 3.3 nM). Compared with paclitaxel, colchicine, vinblastine, and adriamycin, **14h** had much lower drug resistance indexes (1.0 for HCT-8/T, 1.0 for HCT-8/V, 2.3 for MCF-7/ADR, 1.7 for A2780/T) than paclitaxel (567.4 for HCT-8/T and 2042.3 for A2780/T), vinblastine (101.8 for HCT-8/V) and adriamycin (1222.6 for MCF-7/ADR). These results

indicated that **14h** might be useful in the treatment of tumors with resistance to other anti-tubulin drugs.

Table 5. Drug tolerances of **14h** against different drug resistant cancer cells

compd	**IC_{50}[a], nM**		**RR[b]**
	HCT-8	**HCT-8/T**	
14h	3.4 ± 0.2	3.5 ± 0.3	1.0
paclitaxel	17.4 ± 0.1	9885.0 ± 2.8	567.4
compd	**IC_{50}, nM**		**RR**
	HCT-8	**HCT-8/V**	
14h	3.4 ± 0.2	3.5 ± 0.7	1.0
vinblastine	20.2 ± 0.1	2059.0 ± 5.9	101.8
compd	**IC_{50}, nM**		**RR**
	MCF-7	**MCF-7/ADR**	
14h	1.5 ± 0.1	3.3 ± 0.4	2.3
adriamycin	44.8 ± 0.1	54750.0 ± 6.6	1222.1
compd	**IC_{50}, nM**		**RR**
	A2780S	**A2780/T**	
14h	2.2 ± 0.2	3.7 ± 0.5	1.7
paclitaxel	12.3 ± 0.1	25120.0 ± 2.7	2042.3

[a] 50% inhibitory concentration after drug treatment. Data are expressed as the mean ± SD from the dose-response curves of at least three independent experiments.

[b] Resistance ratio: (IC_{50} of drug resistant cancer cell) / (IC_{50} of parental cancer cell).

2.2.3. Cell cycle effects.

To explore whether the cytotoxicity of **14h** was due to the cell cycle arrest, the effect on cell cycle progression was measured using propidium iodide (PI) staining by flow cytometry in A2780S [38]. As depicted in **Figure 2**, **14h** caused a remarkable

G2/M arrest in a concentration-dependent manner. Only 15.34% of the A2780S cells were arrested in G2/M phase in the control group after 24 h treatment, the percentage of G2/M peak increased to 80.67% when cells were exposed to 30 nM of **14h**. The results suggest that **14h** significantly induced cell cycle arrest in the G2/M phase in A2780S cells.

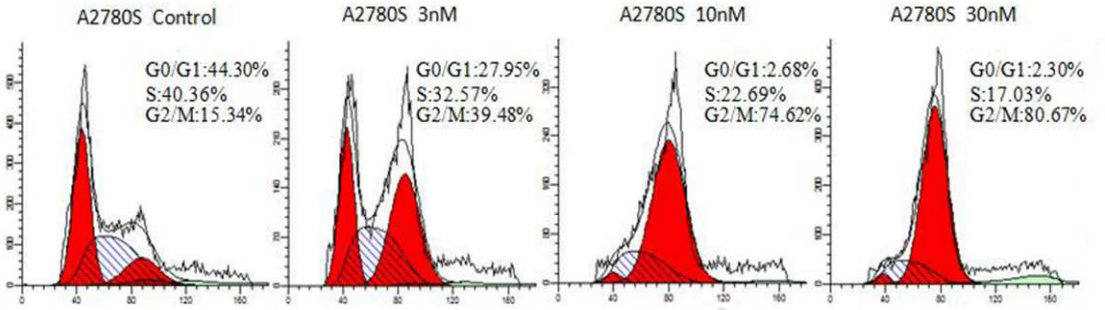

Figure 2. Effects of **14h** on cell cycle phase arrest in A2780S cells. Cells were treated with 3, 10, and 30 nM of **14h** for 24 h.

2.2.4. Immunofluorescence staining.

To investigate whether the antitumor activities of **14h** was derived from an interaction with tubulin, the ability of **14h** to alter the microtubule network was examined by treating with different concentrations of compound **14h** for 24 h and stained for DNA (blue) and α-tubulin (green). The confocal microscopy of A2780S cells shown in **Figure 3** exhibited a well-organized microtubule network in the absence of drug treatment. Treatment with paclitaxel caused the microtubule fibers near the nucleus assemble in clusters. In contrary, cellular microtubules in A2780S cells almost completely depolymerized when exposed to colchicine at 100 nM. **14h** significantly disrupted microtubule formation and exhibited similar effects as

colchicine. In comparison with colchicine, **14h** obviously inhibited microtubules polymerization at 5 nM; moreover **14h** completely disrupted the microtubules polymerization at a concentration of 50 nM. The results suggested that **14h** is most likely targeting tubulin and more active than colchicine as a novel polymerization inhibitor.

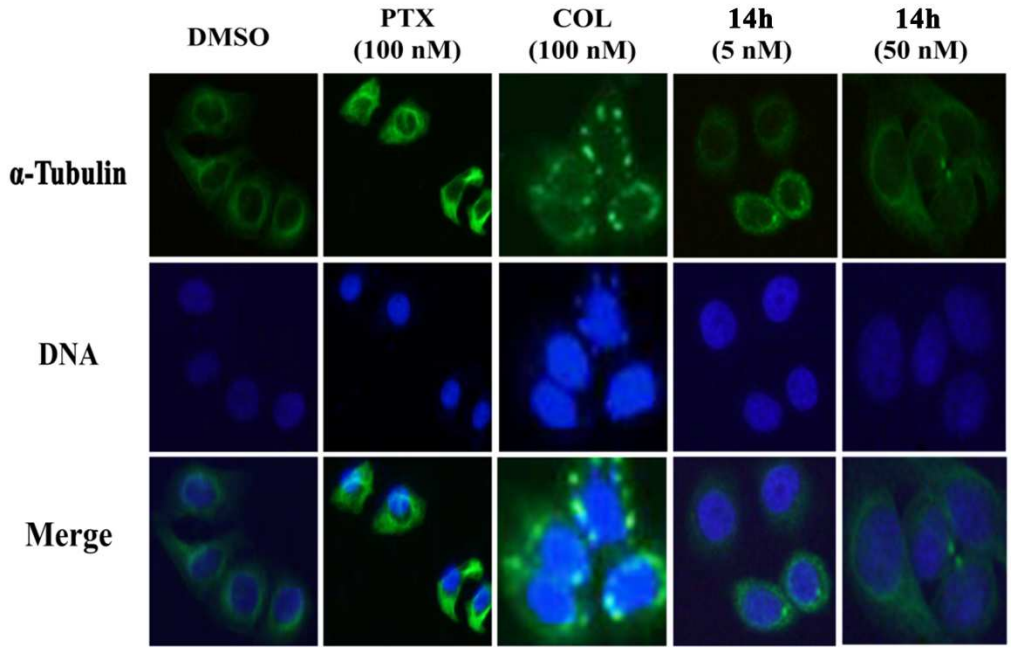

Figure 3. Effects of **14h** on the microtubule network of A2780S cells. A2780S cells were untreated (control) and treated with **14h** (5, 50 nM), paclitaxel (100 nM), or colchicine (100 nM) at the appropriate concentration for 24 h. Microtubules and unassembled tubulin are shown in green and the nuclei in blue.

2.2.5. Effects on microtubule dynamics.

It is well-known that the tubulin binding agents were divided into two types: microtubule stabilizing agents (e.g., paclitaxel) and polymerization inhibitors (e.g., colchicine). **14h** was employed at 0.4, 2, and 10 μM for microtubule dynamics assays

to make clear which type of the compound **14h** related to [39]. (**Figure 4**) Similar but superior to colchicine, **14h** can inhibit tubulin polymerization in a concentration-dependent manner. These data indicated that the mechanism of **14h** was in accordance with polymerization inhibitors, suggesting that compound **14h** might bind to the colchicine site as a novel tubulin depolymerization agent.

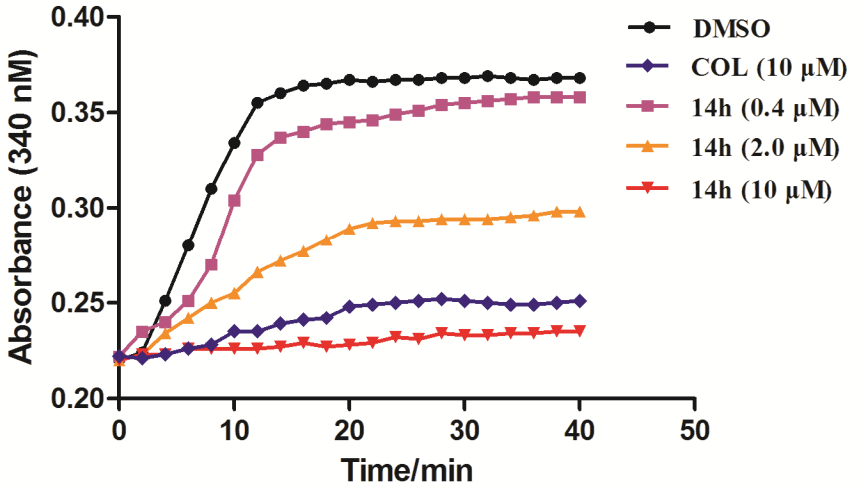

Figure 4. Effect of **14h** on tubulin polymerization assay. Colchicine (10 μM) was used as a reference, while DMSO (0.1% v/v) was used as a vehicle control. Tubulin had been preincubated for 5 min with **14h** at 0.4, 2, and 10 μM at room temperature before GTP was added to start the tubulin polymerization reactions. The reaction was monitored at OD340 nm at 37 °C.

2.2.6. EBI competition assay.

N, *N'*-ethylenebis (iodoacetamide) (EBI), an alkylating agent, specifically cross-link the Cys239 and the Cys354 residues of β-tubulin involved in the colchicine-binding site [40]. An EBI competition assay was carried out in HepG2

cells to confirm whether compound **14h** directly binds to the colchicine binding site. EBI could form a β-tubulin adduct which could be easily detected by Western blot analysis. Antimitotic drugs occupied colchicine-binding site could prevent the formation of the EBI: β-tubulin adduct [40]. Similar to colchicine, compound **14h** (1, 5, and 25 μM) dose-dependently inhibited the formation of the β-tubulin adduct band, resulting in the disappearance of the adduct band. Vincristine has a distinct binding site from colchicine, was used as a negative control (**Figure 5**).

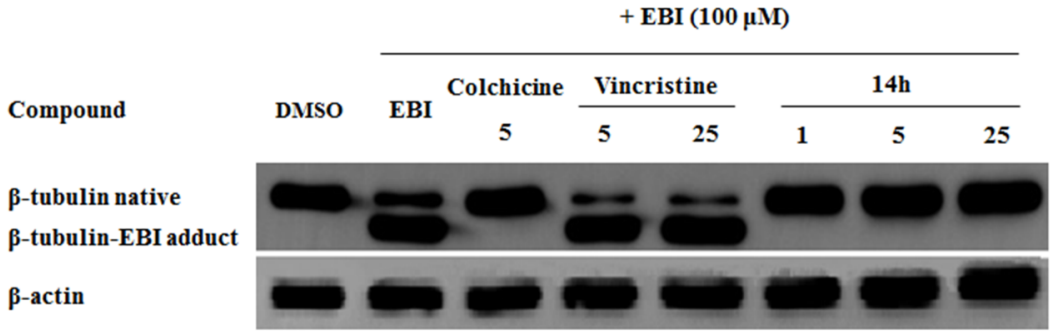

Figure 5. EBI assay: competition assay of **14h** (1, 5, 25 μM), vincristine (5, 25 μM), and colchicine (5 μM) with EBI (100 μM) on HepG2 cells.

2.3. Molecular modeling.

To rationalize our experimental findings, molecular docking simulations of compound **14h** on tubulin were performed using a procedure reported previously [41-45]. The overview of the binding site of **14h** is shown in **Figure 6A**. This binding pocket is located at the interface between the α- and β-subunits of the tubulin dimer; **14h** can enter the pocket like colchicine. The quinoline ring of **14h** forms hydrophobic interactions with the residues of Leu248β, Ala250β, Leu250β, and Ala354β. The tail alkyl chain slightly extends into the α-subunit. (**Figure 6B)** The

right length of the alkyl chain is very important, which may lead to the formation of halogen bond, hydrophobic interactions or other interactions between the chlorine atom of the alkyl chain and the amino acid residues of the α-subunit. This may explain the fact that **14h** is more potent compared to the other compounds.

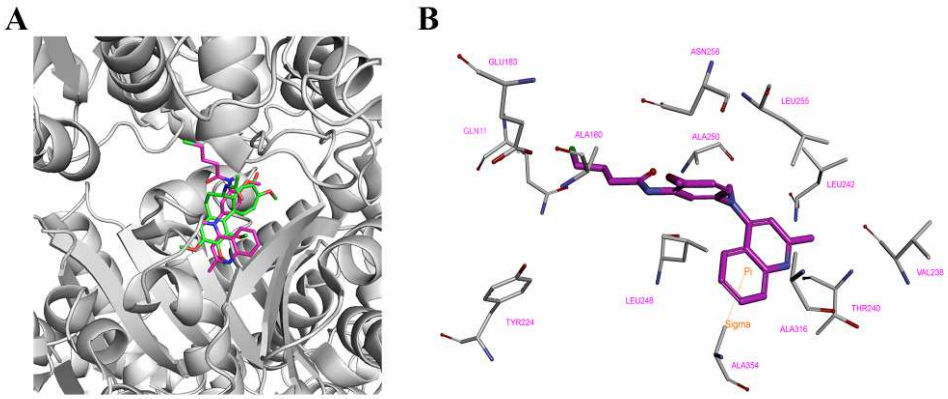

Figure 6. The structures are docked into the colchicine-binding site (PDB code 5eyp) (A) Superimposed molecular models of **14h** (purple) and colchicine (green). (B) Hydrophobic interactions between **14h** and tubulin.

2.4. Animal tumor models and treatment.

HCT116 xenograft model was established in nude mice to determine whether the antitumor ability of **14h** could also be reflected in vivo. HCT116 cells (5×10^6) were inoculated in each flank of null mice. Once the tumor volume reached a size of around 100 mm^3, **14h** was injected at doses of 2.5 mg/kg once every other day. 5-Fluorouracil (5-Fu), as a positive control drug, was administrated every seven days with 100 mg/kg *iv* for comparison [44]. As shown in **Figure 7**, **14h** caused a significant suppression of tumor growth and the average inhibitory rate reached 54.30% at day 18, while 5-Fu at a dosage of 100 mg/kg caused 60.76% tumor reduction. Although 5-Fu at 100mg/kg

showed better antitumor activity than **14h**, the dose is much higher than **14h**. The results demonstrated that **14h** could be used as a potential candidate for cancer treatment. During the therapy, only slight weight loss (<10%) was observed in both of the two drug treatment groups. Serious side-effects, such as feeding and abnormal behavior, were not observed in **14h**-treatment group.

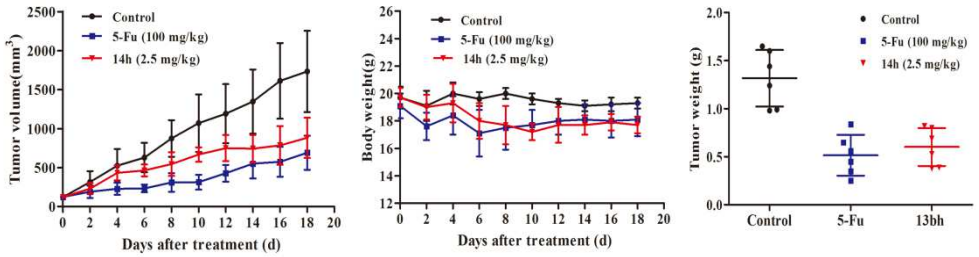

Figure 7. Antitumor effect of **14h** and 5-Fu on the HCT116 xenograft models

3. Conclusion

In our research, 26 novel 4-anilinoquinoline derivatives were synthesized and evaluated for their antiproliferative activities. Among them, compound **14h** exhibited potent antitumor abilities in several human tumor cell lines including multidrug resistant human tumor cell lines, and significantly induced cell cycle arrest in the G2/M phase in A2780S cells. The immunofluorescence assays, microtubule dynamics experiment, EBI assay and molecular modeling studies identified that compound **14h** is a novel depolymerization agent binding to the colchicine site. Then in vivo activity was evaluated on HCT116 xenografts models where compound **14h** showed a favorable effect on inhibiting the tumor growth without significant body weight loss or behavior disorders. Therefore, **14h** as a novel class of tubulin depolymerization agent may be a potent anticancer agent.

4. Experimental

4.1. Chemistry.

All the chemical solvents and reagents used in this study were analytically pure without further purification and commercially available. TLC was performed on 0.20 mm silica gel 60 F_{254} plates (Qingdao Ocean Chemical Factory, Shandong, China). Visualization of spots on TLC plates was done by UV light and I_2. NMR data were measured for ^{1}H at 400 MHz and for ^{13}C at 101 MHz on a Bruker Avance 400 spectrometer (Bruker Company, Germany) using TMS as an internal standard. Mass spectra (MS) were obtained by Q-TOF Priemier mass spectrometer (Micromass, Manchester, UK).

4.1.1. General preparation of **9a-d** (method A).

To a solution of **8a-d** (1.0 equiv) in DMF cooled at 0°C was added sodium hydride (60% oil suspension, 3.0 equiv), followed by methyl iodide (3.0 equiv). The mixture was stirred at 0 °C for 1 h, then allowed to warm to room temperature and stirred for 1 h. The reaction mixture was diluted with ethyl acetate, washed with saturated $NaHCO_3$ aq, brine, dried over Na_2SO_4, filtered and concentrated under vacuum. The residue was purified by flash chromatography using ethyl acetate and petroleum ether (v/v, 1:3) as eluent to give the title compounds **9a-d.**

4.1.1.1. 2-chloro-*N*-(4-methoxyphenyl)-*N*-methylquinolin-4-amine (**9a**).

Compound **9a** was prepared from **8a** (0.33 g, 1.2 mmol), NaH (0.14 g, 3.5 mmol) and CH_3I (0.22 mL, 3.5 mmol) as described for method A as a white solid, yield 57%.

^{1}H NMR (400 MHz, $CDCl_3$) δ 7.96 (dd, *J* = 8.4, 1.2 Hz, 1H), 7.81-7.74 (m, 1H), 7.62-7.56 (m, 1H), 7.29 (t, *J* = 7.6 Hz, 1H), 7.19 (d, *J* = 8.8 Hz, 2H), 6.93 (d, *J* = 9.2 Hz, 2H), 6.71 (s, 1H), 3.86 (s, 3H), 3.56 (s, 3H). ^{13}C NMR (101 MHz, DMSO) δ 158.36, 156.90, 148.63, 141.43, 138.26, 131.33, 128.81, 127.10, 123.94, 123.63, 120.79, 115.86, 111.00, 55.81, 39.08. MS (ESI, m/z): 299.13 $[M + H]^+$.

4.1.1.2. 2-methyl-*N*-(4-methoxyphenyl)-*N*-methylquinolin-4-amine (**9b**).

Compound **9b** was prepared from **8b** (0.13 g, 0.5 mmol), NaH (0.60 g, 1.5 mmol) and CH_3I (0.09 mL, 1.5 mmol) as described for method A as a white solid, yield 52%. ^{1}H NMR (400 MHz, DMSO) δ 7.83 (d, *J* = 8.4 Hz, 1H), 7.56-7.46 (m, 2H), 7.21-7.14 (m, 1H), 7.06 (s, 1H), 6.90 (d, *J* = 9.0 Hz, 2H), 6.83 (d, *J* = 9.0 Hz, 2H), 3.70 (s, 3H), 3.36 (s, 3H), 2.62 (s, 3H). ^{13}C NMR (101 MHz, DMSO) δ 159.62, 155.61, 153.43, 149.57, 144.34, 129.30, 128.96, 125.09, 124.41, 123.74, 121.71, 115.16, 111.95, 55.64, 43.48, 25.55. MS (ESI, m/z): 279.14 [M + H]+.

4.1.1.3. N-(4-methoxyphenyl)-*N*-methylquinolin-4-amine (**9c**).

Compound **9c** was prepared from **8c** (0.25 g, 1.0 mmol), NaH (0.12 g, 3.0 mmol) and CH_3I (0.187 mL, 3.0 mmol) as described for method A as a light yellow solid, yield 56%. ^{1}H NMR (400 MHz, $CDCl_3$) δ 8.74 (d, *J* = 5.2 Hz, 1H), 8.02 (d, *J* = 8.4 Hz, 1H), 7.61 (d, *J* = 8.8 Hz, 1H), 7.57-7.51 (m, 1H), 7.24-7.16 (m, 1H), 6.98 (d, *J* = 5.1 Hz, 1H), 6.91 (d, *J* = 9.0 Hz, 2H), 6.79 (d, *J* = 9.0 Hz, 2H), 3.76 (s, 3H), 3.41 (s, 3H). ^{13}C NMR (101 MHz, DMSO) δ 158.09, 150.86, 148.82, 144.01, 143.57, 140.37, 133.25, 131.27, 129.84, 128.66, 124.12, 122.10, 119.23, 116.58, 107.54, 57.57, 45.24. MS (ESI, m/z): 265.13 $[M + H]^+$.

4.1.1.4. 2-methyl-*N*-(4-(methylthio)phenyl) -*N*-methyl quinolin-4-amine (**9d**).

Compound **9d** was prepared from **8d** (0.14 g, 0.5 mmol), NaH (0.60 g, 1.5 mmol) and CH_3I (0.09 mL, 1.5 mmol) as described for method A as a light yellow solid, yield 49%. ^{1}H NMR (400 MHz, $CDCl_3$) δ 8.00 (d, *J* = 8.4 Hz, 1H), 7.66 (d, *J* = 8.0 Hz, 1H), 7.60 (t, *J* = 7.6 Hz, 1H), 7.32-7.27 (m, 1H), 7.18 (d, *J* = 8.8 Hz, 2H), 7.03 (s, 1H), 6.79 (d, *J* = 8.4 Hz, 2H), 3.43 (s, 3H), 2.71 (s, 3H), 2.44 (s, 3H). ^{13}C NMR (101 MHz, DMSO) δ 160.08, 152.99, 149.61, 147.96, 129.77, 129.45, 128.69, 125.22, 124.57, 122.58, 120.25, 115.34, 42.17, 25.47, 16.44. MS (ESI, m/z): 295.17 $[M + H]^+$.

4.1.2. General preparation of **13a-d** (method B).

To compound **13a-d** (1.0 equiv) in a solution of ethanol and water (v/v 3:1) was added iron powder (5.0 equiv) and ammonium chloride (5.0 equiv). The reaction was stirred at 80 °C for 2 h, then cooled to room temperature, and filtered through Celite. The filter cake was washed with dichloromethane, and the filtrate was concentrated under pressure. The residue was dissolved in dichloromethane, washed with water, dried over Na_2SO_4, filtered, and concentrated. The residue was purified by flash chromatography using ethyl acetate and petroleum ether (v/v, 1:1) as eluent to give the title compounds **13a-d.**

4.1.2.1. *N*-(2-chloroquinolin-4-yl)-4-methoxy-*N*-methylbenzene-1, 3-diamine (**13a**)

Compound **13a** was prepared from **12a** (0.40 g, 1.2 mmol), Fe (0.32 g, 6.0 mmol) and NH_4Cl (0.33 g, 6.0 mmol) as described for method B as a white solid, yield 70%. ^{1}H NMR (400 MHz, DMSO) δ 7.90 (d, *J* = 8.0 Hz, 1H), 7.73-7.59 (m, 2H), 7.36-7.31

(m, 1H), 6.89 (d, *J* = 8.4 Hz, 1H), 6.70 (s, 1H), 6.59 (s, 1H), 6.50 (d, *J* = 8.4 Hz, 1H), 4.98 (s, 2H), 3.82 (s, 3H), 3.43 (s, 3H). ^{13}C NMR (101 MHz, DMSO) δ 157.01, 148.69, 145.66, 141.15, 139.77, 138.64, 131.23, 127.02, 123.91, 123.42, 120.68, 114.44, 112.21, 111.89, 111.29, 55.92, 38.97. MS (ESI, m/z): 314.10 $[M + H]^+$.

4.1.2.2. 4-methoxy-*N*-methyl-*N*-(2-methylquinolin-4-yl)benzene-1,3-diamine (**13b**)

Compound **13b** was prepared from **12b** (6.0 g, 18.5 mmol), Fe (5.2 g, 92.5 mmol) and NH_4Cl (5.0 g, 92.5 mmol) as described for method B as a light yellow solid, yield 78%. ^{1}H NMR (400 MHz, $CDCl_3$) δ 8.48 (d, *J* = 8.0 Hz, 1H), 7.58 (t, *J* = 7.6 Hz, 1H), 7.39 (d, *J* = 8.6 Hz, 1H), 7.14 (t, *J* = 7.6 Hz, 1H), 6.72 (d, *J* = 8.4 Hz, 1H), 6.67 (s, 1H), 6.55 (d, *J* = 2.0 Hz, 1H), 6.41 (dd, *J* = 8.4, 2.1 Hz, 1H), 4.04 (s, 2H), 3.87 (s, 3H), 3.53 (s, 3H), 2.89 (s, 3H). ^{13}C NMR (101 MHz, DMSO) δ 155.35, 144.62, 143.40, 139.44, 132.00, 130.77, 129.14, 126.05, 124.88, 111.68, 109.66, 108.69, 55.95, 44.71, 22.94, 19.13, 14.02. MS (ESI, m/z): 294.15 $[M + H]^+$.

4.1.2.3. 4-methoxy-*N*-methyl-*N*-(quinolin-4-yl)benzene-1,3-diamine (**13c**)

Compound **13c** was prepared from **12c** (0.50 g, 1.6 mmol), Fe (0.45 g, 8.0 mmol) and NH_4Cl (0.43 g, 8.0 mmol) as described for method B as a yellow solid, yield 73%. ^{1}H NMR (400 MHz, DMSO) δ 8.91 (d, *J* = 8.4 Hz, 1H), 8.56 (d, *J* = 7.6 Hz, 1H), 8.12 (s, 2H), 7.85-7.81 (m, 1H), 6.94 (d, *J* = 8.4 Hz, 1H), 6.75-6.65 (m, 2H), 6.58 (d, *J* = 8.0 Hz, 1H), 5.11 (s, 2H), 4.15 (s, 3H), 3.83 (s, 3H). ^{13}C NMR (101 MHz, DMSO) δ 155.52, 147.85, 146.02, 139.59, 139.23, 134.65, 130.32, 127.29, 125.11, 118.96, 118.19, 113.16, 111.50, 110.91, 100.11, 56.04, 42.56. MS (ESI, m/z): 280.40 $[M + H]^+$.

4.1.2.4. 4-methylthio-*N*-methyl-*N*-(2-methylquinolin-4-yl)benzene-1,3-diamine (**13d**)

Compound **13d** was prepared from **12d** (0.40 g, 1.2 mmol), Fe (0.33 g, 6.0 mmol) and NH_4Cl (0.32 g, 6.0 mmol) as described for method B as a light yellow solid, yield 77%. ^{1}H NMR (400 MHz, $CDCl_3$) δ 8.57 (d, *J* = 8.4 Hz, 1H), 7.68-7.57 (m, 1H), 7.41 (d, *J* = 8.8 Hz, 1H), 7.33 (d, *J* = 8.4 Hz, 1H), 7.22-7.15 (m, 1H), 6.76 (s, 1H), 6.57 (d, *J* = 2.3 Hz, 1H), 6.43 (dd, *J* = 8.4, 2.4 Hz, 1H), 4.59 (s, 2H), 3.59 (s, 3H), 2.94 (s, 3H), 2.38 (s, 3H). ^{13}C NMR (101 MHz, DMSO) δ 156.89, 155.23, 149.46, 148.25, 140.40, 133.00, 132.64, 126.47, 125.95, 121.22, 118.74, 118.01, 113.18, 109.98, 108.12, 44.81, 20.62, 16.78. MS (ESI, m/z): 310.20 $[M + H]^+$.

4.1.3. General preparation of **14a-m** (method C).

To a solution of **13b** (0.9 g, 0.34 mmol，1.0 equiv) in dichloromethane (9.0 mL) was added RCO_2Cl (0.41 mmol，1.2 equiv) and triethylamine (0.095 mL, 0.68 mmol, 2.0 equiv), and the mixture stirred at room temperature for 30 min. When completed, the solvent was removed under vacuum and the residue was purified by flash chromatography using dichloromethane and methanol (v/v, 9:1) as eluent to give compounds **14a-m.**

4.1.3.1. *N*-(2-methoxy-5-(methyl(2-methylquinolin-4-yl)amino)phenyl)acetamide (**14a**)

Compound **14a** was prepared from **13b** and acetyl chloride as described for method C as a light yellow solid, yield 41%. ^{1}H NMR (400 MHz, $CDCl_3$) δ 8.42 (s, 1H), 8.18 (d, *J* = 8.0 Hz, 1H), 7.83 (s, 1H), 7.60-7.48 (m, 2H), 7.19-7.11 (m, 1H), 6.83

(s, 1H), 6.69 (d, *J* = 8.8 Hz, 1H), 6.46 (dd, *J* = 8.4, 2.4 Hz, 1H), 3.86 (s, 3H), 3.49 (s, 3H), 2.79 (s, 3H), 2.22 (s, 3H). ^{13}C NMR (101 MHz, DMSO) δ 169.07, 158.67, 154.13, 147.72, 146.32, 143.40, 129.71, 128.82, 127.69, 125.30, 124.73, 121.13, 118.55, 116.82, 112.21, 111.09, 56.36, 43.91, 24.59, 24.37. MS (ESI, m/z): 336.20 $[M + H]^+$.

4.1.3.2. *N*-(2-methoxy-5-(methyl(2-methylquinolin-4-yl)amino)phenyl)propionamide (**14b**)

Compound **14b** was prepared from **13b** and propionyl chloride as described for method C as a light yellow solid, yield 48%. ^{1}H NMR (400 MHz, $CDCl_3$) δ 8.44 (s, 1H), 8.07 (d, *J* = 8.4 Hz, 1H), 7.82 (s, 1H), 7.60-7.50 (m, 2H), 7.19-7.13 (m, 1H), 6.87 (s, 1H), 6.66 (d, *J* = 8.8 Hz, 1H), 6.45-6.37 (m, 1H), 3.86 (s, 3H), 3.46 (s, 3H), 2.75 (s, 3H), 2.45 (q, *J* =7.6 Hz, 2H), 1.28-1.24 (m, 3H). ^{13}C NMR (101 MHz, DMSO) δ 172.69, 158.75, 154.11, 146.23, 143.50, 129.67, 128.85, 125.29, 124.72, 121.19, 118.47, 116.68, 112.20, 111.14, 56.39, 43.94, 29.65, 24.69, 9.99. MS (ESI, m/z): 350.17 $[M + H]^+$.

4.1.3.3. *N*-(2-methoxy-5-(methyl(2-methylquinolin-4-yl)amino)phenyl)butyramide (**14c**)

Compound **14c** was prepared from **13b** and butyryl chloride as described for method C as a light yellow solid, yield 43%. ^{1}H NMR (400 MHz, $CDCl_3$) δ 8.41 (s, 1H), 7.95 (d, *J* = 8.0 Hz, 1H), 7.82 (s, 1H), 7.63 (d, *J* = 8.4 Hz, 1H), 7.51 (t, *J* = 7.6 Hz, 1H), 7.16 (t, *J* = 7.6 Hz, 1H), 6.91 (s, 1H), 6.62 (d, *J* = 8.8 Hz, 1H), 6.35 (d, *J* = 7.2 Hz, 1H), 3.80 (s, 3H), 3.42 (s, 3H), 2.69 (s, 3H), 2.37 (t, *J* = 7.2 Hz, 2H),

1.85-1.66 (m, 2H), 1.01 (t, *J* = 7.6 Hz, 3H). ^{13}C NMR (101 MHz, DMSO) δ 171.81, 159.56, 153.45, 149.48, 145.83, 144.01, 129.24, 129.00, 128.72, 125.03, 124.48, 121.84, 117.93, 116.35, 112.08, 56.35, 43.56, 38.44, 25.52, 18.96, 14.07. MS (ESI, m/z): 364.21 $[M + H]^+$.

4.1.3.4. *N*-(2-methoxy-5-(methyl(2-methylquinolin-4-yl)amino)phenyl)pentanamide (**14d**)

Compound **14d** was prepared from **13b** and pentanoyl chloride as described for method C as a light yellow solid, yield 46%. ^{1}H NMR (400 MHz, $CDCl_3$) δ 8.65 (d, *J* = 8.4 Hz, 1H), 8.54 (s,1 H), 7.90 (s, 1H), 7.62 (t, *J* = 7.6 Hz, 1H), 7.32 (d, *J* = 8.4 Hz, 1H), 7.16 (t, *J* = 7.6 Hz, 1H), 6.82 (d, *J* = 8.4 Hz, 1H), 6.75-6.62 (m, 2H), 3.96 (s, 3H), 3.62 (s, 3H), 2.98 (s, 3H), 2.44 (t, *J* = 7.6 Hz, 2H), 1.76-1.66 (m, 2H), 1.47-1.36 (m, 2H), 0.95 (t, *J* = 7.2 Hz, 3H). ^{13}C NMR (101 MHz, DMSO) δ 172.34, 157.22, 154.60, 148.62, 140.78, 139.69, 132.80, 129.41, 126.54, 125.84, 121.33, 120.53, 118.77, 117.97, 112.61, 106.78, 56.55, 45.67, 36.17, 27.60, 22.24, 20.19, 14.20. MS (ESI, m/z): 378.25 $[M + H]^+$.

4.1.3.5. *N*-(2-methoxy-5-(methyl(2-methylquinolin-4-yl)amino)phenyl)acrylamide (**14e**)

Compound **14e** was prepared from **13b** and acryloyl chloride as described for method C as a light yellow solid, yield 46%. ^{1}H NMR (400 MHz, DMSO) δ 9.35 (s, 1H), 7.87 (s, 1H), 7.82 (d, *J* = 8.8 Hz, 1H), 7.55-7.46 (m, 2H), 7.22-7.16 (m, 1H), 7.08 (s, 1H), 6.95 (d, *J* = 8.8 Hz, 1H), 6.73-6.60 (m, 2H), 6.15 (dd, *J* = 16.8, 2.0 Hz, 1H), 5.72-5.62 (m, 1H), 3.80 (s, 3H), 3.36 (s, 3H), 2.62 (s, 3H). ^{13}C NMR (101 MHz,

DMSO) δ 164.04, 157.23, 154.72, 148.86, 140.87, 139.79, 132.78, 132.17, 129.03, 127.69, 126.53, 125.88, 121.86, 120.62, 119.13, 118.07, 112.76, 106.97, 56.62, 20.23. MS (ESI, m/z): 348.05 $[M + H]^+$.

4.1.3.6.

2-chloro-*N*-(2-methoxy-5-(methyl(2-methylquinolin-4-yl)amino)phenyl)acetamide (**14f**)

Compound **14f** was prepared from **13b** and 2-chloroacetyl chloride as described for method C as a light yellow solid, yield 47%. ^{1}H NMR (400 MHz, DMSO) δ 9.48 (s, 1H), 7.88-7.74 (m, 2H), 7.59-7.47 (m, 2H), 7.20 (t, *J* = 7.2 Hz, 1H), 7.09 (s, 1H), 6.97 (t, *J* = 8.4 Hz, 1H), 6.74-6.62 (m, 1H), 4.34 (s, 2H), 3.81 (s, 3H), 3.36 (s, 3H), 2.63 (s, 3H). ^{13}C NMR (101 MHz, DMSO) δ 165.28, 158.94, 153.93, 148.12, 146.15, 143.64, 129.62, 127.99, 125.16, 124.80, 121.35, 118.99, 116.17, 112.46, 111.67, 56.53, 43.79, 24.81. MS (ESI, m/z): 370.20 $[M + H]^+$.

4.1.3.7.

3-chloro-*N*-(2-methoxy-5-(methyl(2-methylquinolin-4-yl)amino)phenyl)propanamide (**14g**)

Compound **14g** was prepared from **13b** and 3-chloropropanoyl chloride as described for method C as a light yellow solid, yield 45%. ^{1}H NMR (400 MHz, $CDCl_3$) δ 8.39 (s, 1H), 8.03 (d, *J* = 8.0 Hz, 1H), 7.92 (s, 1H), 7.59 (d, *J* = 8.4 Hz, 1H), 7.54 (t, *J* = 7.6 Hz, 1H), 7.18 (t, *J* = 7.6 Hz, 1H), 6.89 (s, 1H), 6.67 (d, *J* = 8.8 Hz, 1H), 6.42 (d, *J* = 8.8 Hz, 1H), 3.89 (t, *J* = 6.4 Hz, 2H), 3.85 (s, 3H), 3.44 (s, 3H), 2.87 (t, *J* = 6.4 Hz, 2H), 2.73 (s, 3H). ^{13}C NMR (101 MHz, DMSO) δ 164.02, 157.00, 155.09, 148.64,

141.09, 132.57, 132.18, 128.99, 127.68, 126.45, 125.80, 121.59, 118.90, 118.34, 112.72, 107.35, 56.61, 45.45, 20.70. MS (ESI, m/z): 384.18 $[M + H]^+$.

4.1.3.8.

4-chloro-*N*-(2-methoxy-5-(methyl(2-methylquinolin-4-yl)amino)phenyl)butanamide (**14h**)

Compound **14h** was prepared from **13b** and 4-chlorobutanoyl chloride as described for method C as a light yellow solid, yield 49%. ^{1}H NMR (400 MHz, $CDCl_3$) δ 8.35 (d, *J* = 2.4 Hz, 1H), 7.96 (d, *J* = 8.4 Hz, 1H), 7.84 (s, 1H), 7.62 (dd, *J* = 8.4, 0.8 Hz, 1H), 7.55-7.50 (m, 1H), 7.20-7.15 (m, 1H), 6.92 (s, 1H), 6.65 (d, *J* = 8.8 Hz, 1H), 6.38 (dd, *J* = 8.8, 2.4 Hz, 1H), 3.83 (s, 3H), 3.67 (t, *J* = 6.4 Hz, 2H), 3.43 (s, 3H), 2.70 (s, 3H), 2.61 (t, *J* = 6.8 Hz, 2H), 2.26-2.15 (m, 2H). ^{13}C NMR (101 MHz, $CDCl_3$) δ 169.92, 159.15, 154.13, 148.99, 144.01, 143.70, 129.02, 128.47, 124.97, 124.35, 121.93, 116.90, 113.69, 112.14, 110.42, 55.97, 44.43, 42.96, 34.38, 27.85, 25.26. MS (ESI, m/z): 398.34 $[M + H]^+$.

4.1.3.9.

5-chloro-*N*-(2-methoxy-5-(methyl(2-methylquinolin-4-yl)amino)phenyl)pentanamide (**14i**)

Compound **14i** was prepared from **13b** and 5-chloropentanoyl chloride as described for method C as a light yellow solid, yield 47%. ^{1}H NMR (400 MHz, DMSO) δ 9.05 (s, 1H), 7.82 (d, *J* = 8.4 Hz, 2H), 7.52 (t, *J* = 7.6 Hz, 2H), 7.19 (t, *J* = 7.6 Hz, 1H), 7.06 (s, 1H), 6.90 (d, *J* = 8.8 Hz, 1H), 6.62 (dd, *J* = 8.6, 2.0 Hz, 1H), 3.80 (s, 3H), 3.63 (t, *J* = 9.0 Hz, 2H), 3.35 (s, 3H), 2.62 (s, 3H), 2.38 (t, *J* = 7.2 Hz,

2H), 1.74-1.68 (m, 2H), 1.66-1.60 (m, 2H). ^{13}C NMR (101 MHz, DMSO) δ 171.64, 158.78, 154.04, 146.33, 143.49, 129.63, 128.74, 127.88, 125.27, 124.71, 121.23, 118.54, 116.79, 112.24, 111.24, 56.40, 45.54, 43.89, 35.51, 31.99, 24.73, 22.84. MS (ESI, m/z): 412.20 $[M + H]^+$.

4.1.3.10.

2-bromo-*N*-(2-methoxy-5-(methyl(2-methylquinolin-4-yl)amino)phenyl)acetamide (**14j**)

Compound **14j** was prepared from **13b** and 2-bromoacetyl bromide as described for method C as a light yellow solid, yield 53%. ^{1}H NMR (400 MHz, DMSO) δ 9.59 (s, 1H), 7.85-7.78 (m, 2H), 7.59-7.47 (m, 2H), 7.25-7.17 (m, 1H), 7.09 (s, 1H), 6.96 (d, *J* = 8.8 Hz, 1H), 6.69 (dd, *J* = 8.4, 2.4 Hz, 1H), 4.16 (s, 2H), 3.81 (s, 3H), 3.37 (s, 3H), 2.63 (s, 3H). ^{13}C NMR (101 MHz, DMSO) δ 171.09, 157.36, 154.66, 147.42, 141.00, 139.57, 133.11, 128.54, 126.61, 126.02, 121.35, 120.48, 117.89, 116.13, 112.66, 106.84, 56.89, 45.78, 20.48. MS (ESI, m/z): 414.20 $[M + H]^+$.

4.1.3.11.

Methyl-2-((2-methoxy-5-(methyl(2-methylquinolin-4-yl)amino)phenyl)amino)-2-oxo acetate (**14k**)

Compound **14k** was prepared from **13b** and methyl 2-chloro-2-oxoacetate as described for method C as a light yellow solid, yield 56%. ^{1}H NMR (400 MHz, $CDCl_3$) δ 9.48 (s, 1H), 8.35 (d, *J* = 2.8 Hz, 1H), 8.03 (s, 1H), 7.61-7.54 (m, 2H), 7.22-7.15 (m, 1H), 6.93 (s, 1H), 6.71 (d, *J* = 8.8 Hz, 1H), 6.50 (dd, *J* = 8.8 Hz, *J* = 2.4 Hz, 1H), 3.97 (s, 3H), 3.88 (s, 3H), 3.46 (s, 3H), 2.74 (s, 3H). ^{13}C NMR (101 MHz, DMSO) δ

161.22, 159.06, 155.09, 153.82, 145.96, 143.71, 129.67, 128.20, 126.70, 124.99, 121.46, 119.44, 115.26, 112.60, 112.21, 56.69, 53.81, 43.59, 24.85. MS (ESI, m/z): 380.15 $[M + H]^+$.

4.1.3.12. Ethyl-2-((2-methoxy-5-(methyl(2-methylquinolin-4-yl)amino)phenyl)amino) -2-oxoacetate (**14l**)

Compound **14l** was prepared from **13b** and ethyl 2-chloro-2-oxoacetate as described for method C as a light yellow solid, yield 65%. ^{1}H NMR (400 MHz, $CDCl_3$) δ 9.50 (s, 1H), 8.35 (d, *J* = 2.8 Hz, 1H), 8.02 (d, *J* = 8.0 Hz, 1H), 7.61 (d, *J* = 8.4 Hz, 1H), 7.57-7.52 (m, 1H), 7.20 (t, *J* = 7.6 Hz, 1H), 6.93 (s, 1H), 6.71 (d, *J* = 8.8 Hz, 1H), 6.49 (dd, *J* = 8.8, 2.4 Hz, 1H), 4.41 (q, *J* = 7.2 Hz, 2H), 3.87 (s, 3H), 3.45 (s, 3H), 2.73 (s, 3H), 1.42 (t, *J* = 7.2 Hz, 3H). ^{13}C NMR (101 MHz, DMSO) δ 160.74, 159.37, 155.17, 153.57, 145.73, 143.93, 129.43, 128.75, 126.67, 124.90, 121.73, 119.11, 114.99, 112.57, 63.09, 56.69, 43.43, 25.18, 14.22. MS (ESI, m/z): 394.11 $[M + H]^+$.

4.1.3.13.

Methyl-5-((2-methoxy-5-(methyl(2-methylquinolin-4-yl)amino)phenyl)amino)-5-oxo pentanoate (**14m**)

Compound **14m** was prepared from **13b** and methyl 5-chloro-5-oxopentanoate as described for method C as a light yellow solid, yield 47%. ^{1}H NMR (400 MHz, DMSO) δ 9.05 (s, 1H), 7.85-7.76 (m, 2H), 7.56-7.48 (m, 2H), 7.21-7.16 (m, 1H), 7.06 (s, 1H), 6.90 (d, *J* = 8.8 Hz, 1H), 6.61 (dd, *J* = 8.8, 2.4 Hz, 1H), 3.78 (s, 3H), 3.57 (s, 3H), 3.35 (s, 3H), 2.62 (s, 3H), 2.38 (t, *J* = 7.2 Hz, 2H), 2.31 (t, *J* = 7.6 Hz, 2H),

1.82-1.71 (m, 2H). ^{13}C NMR (101 MHz, DMSO) δ 173.49, 171.31, 159.51, 153.48, 149.39, 145.93, 143.98, 129.11, 128.62, 125.03, 124.50, 121.80, 118.06, 116.49, 112.08, 56.35, 51.68, 43.56, 35.47, 33.11, 25.48, 20.84. MS (ESI, m/z): 422.26 [M + H]$^+$.

4.1.4. General preparation of **14a-e** (method D).

To a solution of compound **14f** (90 mg, 0.27mmol, 1.0 equiv) in acetonitrile heated at 80°C was added 3-methylaminopropionitrile (0.32mmol, 1.2 equiv) and potassium carbonate (0.54mmol, 2.0 equiv) refluxed for 2h. The reaction mixture was cooled and the solvent removed under reduced pressure. The residue was partitioned between brine and ethyl acetate. The aqueous layer was extracted with ethyl acetate. The combined organics were dried over Na_2SO_4 and concentrated. The residue was purified by flash chromatography using dichloromethane and methanol (v/v, 9:1) as eluent to give the product **15a**. Under the same conditions, **15b-e** can be obtained by replacing 3-methylaminopropionitrile with different amines.

4.1.4.1. 2-((2-cyanoethyl)(methyl)amino)-*N*-(2-methoxy-5-(methyl(2-methylquinolin-4-yl)amino)phenyl)acetamide (**15a**)

Compound **15a** was prepared from **14f** and 3-methylaminopropionitrile as described for method D as a light yellow solid, yield 66%. ^{1}H NMR (400 MHz, $CDCl_3$) δ 9.55 (s, 1H), 8.36 (d, *J* = 2.8 Hz, 1H), 7.98 (d, *J* = 8.0 Hz, 1H), 7.62 (d, *J* = 7.6 Hz, 1H), 7.55-7.50 (m, 1H), 7.20-7.14 (m, 1H), 6.91 (s, 1H), 6.67 (d, *J* = 8.8 Hz, 1H), 6.42 (dd, *J* = 8.4, 2.8 Hz, 1H), 3.85 (s, 3H), 3.44 (s, 3H), 3.24 (s, 2H), 2.87 (t, *J* =

6.7 Hz, 2H), 2.72 (s, 3H), 2.59 (t, *J* = 6.7 Hz, 2H), 2.47 (s, 3H). ^{13}C NMR (101 MHz, DMSO) δ 168.77, 159.61, 153.41, 149.53, 144.65, 144.23, 129.31, 129.03, 128.24, 124.96, 124.56, 121.92, 120.00, 117.48, 113.68, 112.29, 111.92, 61.54, 56.48, 52.76, 43.54, 42.61, 25.55, 16.30. MS (ESI, m/z): 418.27 $[M + H]^+$.

4.1.4.2.

N-(2-methoxy-5-(methyl(2-methylquinolin-4-yl)amino)phenyl)-2-(3-methylpiperidin-1-yl)acetamide (**15b**)

Compound **15b** was prepared from **14f** and 3-methylpiperidine as described for method D as a light yellow solid, yield 74%. ^{1}H NMR (400 MHz, $CDCl_3$) δ 9.96 (s, 1H), 8.42 (d, *J* = 2.6 Hz, 1H), 8.01 (d, *J* = 7.8 Hz, 1H), 7.62 (d, *J* = 8.4 Hz, 1H), 7.53 (t, *J* = 7.6 Hz, 1H), 7.17 (t, *J* = 7.6 Hz, 1H), 6.90 (s, 1H), 6.65 (dd, *J* = 8.8Hz, 2.4Hz, 1H), 6.38 (dd, *J* = 8.8, 2.4 Hz, 1H), 3.85 (d, *J* = 8.4 Hz, 3H), 3.45 (s, 3H), 3.09 (s, 2H), 2.80 (d, *J* = 9.8 Hz, 2H), 2.73 (s, 3H), 2.22 (t, *J* = 9.0 Hz, 1H), 1.95 (t, *J* = 9.4 Hz, 1H), 1.84-1.54 (m, 5H), 0.93 (d, *J* = 6.4 Hz, 3H). ^{13}C NMR (101 MHz, DMSO) δ 168.80, 159.59, 153.42, 149.50, 144.37, 129.28, 129.05, 128.31, 124.95, 124.57, 121.92, 117.21, 113.15, 112.01, 62.38, 61.71, 56.65, 54.12, 43.51, 32.18, 31.48, 25.53, 22.54, 19.56. MS (ESI, m/z): 433.06 $[M + H]^+$.

4.1.4.3.

N-(2-methoxy-5-(methyl(2-methylquinolin-4-yl)amino)phenyl)-2-morpholinoacetamide (**15c**)

Compound **15c** was prepared from **14f** and morpholine as described for method D as a light yellow solid, yield 71%. ^{1}H NMR (400 MHz, $CDCl_3$) δ 9.82 (s, 1H), 8.37

(d, *J* = 2.6 Hz, 1H), 7.97 (d, *J* = 8.4 Hz, 1H), 7.62 (d, *J* = 8.4 Hz, 1H), 7.53 (t, *J* = 7.6 Hz, 1H), 7.15 (t, *J* = 7.6 Hz, 1H), 6.91 (s, 1H), 6.66 (d, *J* = 8.8 Hz, 1H), 6.39 (dd, *J* = 8.8, 2.4 Hz, 1H), 3.86 (s, 3H), 3.83-3.77 (m, 4H), 3.44 (s, 3H), 3.16 (s, 2H), 2.71 (s, 3H), 2.68-2.61 (m, 4H). ^{13}C NMR (101 MHz, DMSO) δ 168.24, 159.59, 153.41, 149.47, 144.42, 129.16, 128.21, 124.94, 124.58, 121.91, 117.35, 113.35, 112.36, 112.06, 66.98, 62.03, 56.74, 53.59, 43.51, 25.52. MS (ESI, m/z): 421.16 $[M + H]^+$.

4.1.4.4.

N-(2-methoxy-5-(methyl(2-methylquinolin-4-yl)amino)phenyl)-2-thiomorpholinoacetamide (**15d**)

Compound **15d** was prepared from **14f** and thiomorpholine as described for method D as a light yellow solid, yield 69%. ^{1}H NMR (400 MHz, $CDCl_3$) δ 9.77 (s, 1H), 8.37 (d, *J* = 2.8 Hz, 1H), 8.02 (d, *J* = 8.4 Hz, 1H), 7.60 (d, *J* = 8.4 Hz, 1H), 7.53 (t, *J* = 7.2 Hz, 1H), 7.17 (t, *J* = 7.2 Hz, 1H), 6.90 (s, 1H), 6.68 (d, *J* = 8.8 Hz, 1H), 6.41 (dd, *J* = 8.8, 2.6 Hz, 1H), 3.88 (s, 3H), 3.45 (s, 3H), 3.15 (s, 2H), 2.92-2.84 (m, 4H), 2.81-2.75 (m, 4H), 2.73 (s, 3H). ^{13}C NMR (101 MHz, DMSO) δ 168.48, 158.53, 154.24, 145.14, 143.63, 129.93, 128.30, 127.43, 125.30, 124.88, 121.05, 118.19, 113.94, 112.15, 111.17, 62.52, 56.80, 55.10, 44.00, 31.43, 28.11, 24.48. MS (ESI, m/z): 437.25 $[M + H]^+$.

4.1.4.5.

N-(2-methoxy-5-(methyl(2-methylquinolin-4-yl)amino)phenyl)-2-((2-(phenylamino)ethyl)amino)acetamide (**15e**)

Compound **15e** was prepared from **14f** and N^1-phenylethane-1, 2-diamine as described for method D as a light yellow solid, yield 69%. ^{1}H NMR (400 MHz, $CDCl_3$) δ 9.76 (s, 1H), 8.44 (d, *J* = 2.4 Hz, 1H), 8.11 (d, *J* = 8.0 Hz, 1H), 7.51-7.60 (m, 2H), 7.15-7.21 (m, 3H), 6.87 (s, 1H), 6.77-6.61 (m, 4H), 6.45 (dd, *J* = 8.8, 2.4 Hz, 1H), 3.87 (s, 3H), 3.48 (s, 3H), 3.46 (s, 2H), 3.33 (t, *J* = 5.6 Hz, 2H), 2.96 (t, *J* = 5.6 Hz, 2H), 2.77 (s, 3H). ^{13}C NMR (101 MHz, DMSO) δ 169.79, 159.50, 153.51, 149.26, 144.79, 144.23, 129.38, 129.12, 128.25, 125.00, 124.59, 121.84, 117.51, 116.23, 113.85, 112.48, 112.12, 56.56, 52.61, 48.58, 43.56, 43.03, 25.44. MS (ESI, m/z): 470.37 $[M + H]^+$.

4.2. Biological assay methods.

4.2.1. Cell proliferation assay.

The anti-proliferation activities of the compounds were tested in HCT116 cells, A549 cells, A2780S cells, A2780/T cells，HCT-8 cells, HCT-8/T cells, HCT-8/V cells，MDA-MB-231 cells, MCF-7 cells, and MCF-7/ADR cells. Cells in logarithmic phase were seeded in 96-well plates and allowed to adhere. Then the cells were incubated with indicated concentrations of the compounds for 48 h. MTT was subsequently added for an extra 2-3 h of incubation. The MTT formazan precipitate was dissolved in DMSO, and the absorbance was measured at a wavelength of 570 nm by a Spectramax M5 microtiter plate luminometer (Molecular Devices, Sunnyvale, CA, USA).

4.2.2. Flow cytometry.

A2780S cells were incubated with various concentrations of selected compound or DMSO vehicle for 24 h at 37 °C. The cells were washed by PBS, and then the cell DNA was stained with 50 μg/mL PI containing 1 mg/mL of DNase-free RNaseA for a minimum of 9 min. The samples were analyzed by a flow cytometer (BD FACS Calibur, Franklin Lakes, NJ, USA).

4.2.3. Immunofluorescence staining.

The immunofluorescence study of microtubule system was conducted generally as describe. A2780S cells were seeded into 96-well plates and then treated with the selected compound, paclitaxel, colchicine, and DMSO as indicated for 24 h. The cells were fixed with 4% paraformaldehyde and then penetrated with PBS containing 0.5% Triton X-90. After blocking for 30 min in 5% goat serum albumin at room temperature, cells were incubated with a monoclonal antibody (anti-α-tubulin) at room temperature for 1 h. Then the cells were washed three times by PBS following staining by fluorescence antibody and labeling of nuclei by DAPI. Cells were finally washed thrice and visualized using a fluorescence microscope (OLYMPUS, Tokyo, Japan).

4.2.4. In vitro tubulin polymerization assay.

An amount of 2 mg/mL tubulin (Cytoskeleton) resuspended in PEM buffer [80 mM PIPES (pH 6.9), 0.5 mM EGTA, 2 mM $MgCl_2$, and 15% glycerol] and then was preincubated with compounds or vehicle DMSO on ice. PEG containing GTP was added to the final concentration of 3 mg/mL before detecting the tubulin polymerization reaction. The reaction was monitored by a spectrophotometer in

absorbance at 340 nm at 37 °C every 2 min. The final concentrations of the compound were list as follows: **14h** (0.2, 2, and 9 μM), colchicine (9 μM).

4.2.5. EBI Competition Assay.

Six-well plates were seeded with HepG2 cells at 5×9^5 cells per well. Cells were first incubated with compound **14h** (1, 5, and 25 μM), vincristine (5 and 25 μM), or colchicine (5 μM) for 2 h and afterward treated with EBI (100 μM). After 1.5 h, the cells were harvested and cell extracts were prepared for Western blot analysis. An amount of 20 μg of proteins was subjected to gel electrophoresis using 9% polyacrylamide gels. The proteins were transferred onto PVDF membranes, then blocked by 5% nonfat milk for 1 h, and subsequently incubated with anti-β-tubulin antibody (Cell Signaling Technology, no. 2146) for 16 h at 4 °C. Next, the membranes were washed extensively. Immunoreactive proteins were finally detected by chemiluminescence (Millipore, USA). β-actin was also examined to approve equal loading of protein.

4.2.6. Molecular docking.

Tubulin was chosen as the target receptor. The 3D structure of the receptor was gained from Protein Data Bank. The docking procedure was performed in Discovery Studio 3.1 package. In the process of docking, proteins were prepared by Discovery Studio modules, all water molecules were eliminated, all atoms within 9 Å of ligands were defined as binding site, and Goldscore was chosen as the fitting function

4.2.7. Animal tumor models and treatment.

We established HCT116 in vivo xenograft model in a method similar as described. We used 5-to-6-week-old female Balb/C and athymic nude mice, respectively, and implanted the indicated number of cells suspended in 90 CE HBSS in the right flank of mice. When tumor volumes reached 90 mm^3, the animals were treated with vehicle (containing 2.5% Tween-80 and 2.5% ethanol), 5-Fu (90 mg/kg, every 7 days), or **14h** (2.5 mg/kg, every 2 days). Signs of toxicity and mortality were observed daily. Tumor volumes and body weights were measured every 2 days when administrated with a caliper (calculated volume (mm^3) = (π/6) × length × width × width). The antitumor activity of compound was evaluated by tumor inhibitor = (1 - tumor weight of treated group/tumor weight of control group) × 90%.

Acknowledgments

The authors greatly appreciate the financial support from National Natural Science Foundation of China (Grant U1402222).

Abbreviations Used

EBI, *N*, *N*'-ethylenebis (iodoacetamide); CA-4, combretastatin A-4; FDA, Food and Drug Administration; EMA, European Medicines Agency; DMF, N, N-Dimethylformamide; MTT, 3-(4,5-dimethylthiazol-2-yl)-2,5-diphenyltetrazolium bromide; ADM, Adriamycin; PTX, paclitaxel; COL, colchicine; iv, intravenous.

REFERENCES

[1] K.H. Downing, E. Nogales, Tubulin and microtubule structure, Current Opinion in Cell Biology, 10 (1998).

[2] E.A. Perez, Microtubule inhibitors: Differentiating tubulin-inhibiting agents based on mechanisms of action, clinical activity, and resistance, Molecular cancer therapeutics, 8 (2009) 2086-2095.

[3] C. Dumontet, M.A. Jordan, Microtubule-binding agents: a dynamic field of cancer therapeutics, Nature reviews. Drug discovery, 9 (2010) 790-803.

[4] S. Sharma, C. Kaur, A. Budhiraja, K. Nepali, M.K. Gupta, A.K. Saxena, P.M. Bedi, Chalcone based azacarboline analogues as novel antitubulin agents: design, synthesis, biological evaluation and molecular modelling studies, European journal of medicinal chemistry, 85 (2014) 648-660.

[5] F. Pellegrini, D.R. Budman, Review: Tubulin Function, Action of Antitubulin Drugs, and New Drug Development, Cancer Investigation, 23 (2005) 264-273.

[6] C. Vilanova, S. Torijano-Gutierrez, S. Diaz-Oltra, J. Murga, E. Falomir, M. Carda, J. Alberto Marco, Design and synthesis of pironetin analogue/combretastatin A-4 hybrids containing a 1,2,3-triazole ring and evaluation of their cytotoxic activity, European journal of medicinal chemistry, 87 (2014) 125-130.

[7] A. Kamal, A.B. Shaik, N. Jain, C. Kishor, A. Nagabhushana, B. Supriya, G. Bharath Kumar, S.S. Chourasiya, Y. Suresh, R.K. Mishra, A. Addlagatta, Design and synthesis of pyrazole-oxindole conjugates targeting tubulin polymerization as new anticancer agents, European journal of medicinal chemistry, 92 (2015) 501-513.

[8] Y. Wang, H. Zhang, B. Gigant, Y. Yu, Y. Wu, X. Chen, Q. Lai, Z. Yang, Q. Chen, J. Yang, Structures of a diverse set of colchicine binding site inhibitors in complex

with tubulin provide a rationale for drug discovery, The FEBS journal, 283 (2016) 102-111.

[9] A.E. Prota, K. Bargsten, J.F. Diaz, M. Marsh, C. Cuevas, M. Liniger, C. Neuhaus, J.M. Andreu, K.H. Altmann, M.O. Steinmetz, A new tubulin-binding site and pharmacophore for microtubule-destabilizing anticancer drugs, Proceedings of the National Academy of Sciences of the United States of America, 111 (2014) 13817-13821.

[10] J.M. Andreu, I. Barasoain, The Interaction of Baccatin III with the Taxol Binding Site of Microtubules Determined by a Homogeneous Assay with Fluorescent Taxoid, Biochemistry, (2001).

[11] S.S. Rai, J. Wolff, Localization of the Vinblastine-binding Site on b-Tubulin, J. Biol. Chem. , 271 (1996) 14707.

[12] E.t. Haar, H.S. Rosenkranz, E. Hamel, B.W. Day, Computational and Molecular Modeling Evaluation of the Structural Basis for Tubulin Polymerization Inhibition by Colchicine Site Agents, Bioorganic & medicinal chemistry, 4 (1996).

[13] G.D. Leonard, T. Fojo, S.E. Bates, The role of ABC transporters in clinical practice., Oncologist, 8 (2003) 411-424.

[14] T. Fojo, M. Menefee, Mechanisms of multidrug resistance: the potential role of microtubule-stabilizing agents, Annals of oncology : official journal of the European Society for Medical Oncology, 18 Suppl 5 (2007) v3-8.

[15] P.D.W. Eckford, F.J. Sharom, ABC Efflux Pump-Based Resistance to Chemotherapy Drugs, Chem. Rev, 109 (2009).

[16] G.R. Pettit, S.B. Singh, E. Hamel, C.M. Lin, D.S. Alberts, D. Garcia-Kendall, Isolation and structure of the strong cell growth and tubulin inhibitor combretastatin A-4 Experientia, 45 (1988) 680.

[17] M. Zweifel, G.C. Jayson, N.S. Reed, R. Osborne, B. Hassan, J. Ledermann, G. Shreeves, L. Poupard, S.P. Lu, J. Balkissoon, D.J. Chaplin, G.J. Rustin, Phase II trial of combretastatin A4 phosphate, carboplatin, and paclitaxel in patients with platinum-resistant ovarian cancer, Annals of oncology : official journal of the European Society for Medical Oncology, 22 (2011) 2036-2041.

[18] G.J. Rustin, G. Shreeves, P.D. Nathan, A. Gaya, T.S. Ganesan, D. Wang, J. Boxall, L. Poupard, D.J. Chaplin, M.R. Stratford, J. Balkissoon, M. Zweifel, A Phase Ib trial of CA4P (combretastatin A-4 phosphate), carboplatin, and paclitaxel in patients with advanced cancer, British journal of cancer, 102 (2010) 1355-1360.

[19] D. Cao, Y. Liu, W. Yan, C. Wang, P. Bai, T. Wang, M. Tang, X. Wang, Z. Yang, B. Ma, L. Ma, L. Lei, F. Wang, B. Xu, Y. Zhou, T. Yang, L. Chen, Design, Synthesis, and Evaluation of in Vitro and in Vivo Anticancer Activity of 4-Substituted Coumarins: A Novel Class of Potent Tubulin Polymerization Inhibitors, Journal of medicinal chemistry, 59 (2016) 5721-5739.

[20] W.A. Denny, DNA minor groove alkylating agents, Curr Med Chem, 8 (2001) 533-544.

[21] S.K. Rabindran, C.M. Discafani, E.C. Rosfjord, M. Baxter, M.B. Floyd, J. Golas, W.A. Hallett, B.D. Johnson, R. Nilakantan, E. Overbeek, M.F. Reich, R. Shen, X. Shi, H.-R. Tsou, Y.-F. Wang, A. Wissner, Antitumor activity of HKI-272, an orally active, irreversible inhibitor of the HER-2 tyrosine kinase, Cancer research, 64 (2004) 3958-3965.

[22] F.A.L.M. Eskens, M.J.A. de Jonge, P. Bhargava, T. Isoe, M.M. Cotreau, B. Esteves, K. Hayashi, H. Burger, M. Thomeer, L. van Doorn, J. Verweij, Biologic and clinical activity of tivozanib (AV-951, KRN-951), a selective inhibitor of VEGF receptor-1, -2, and -3 tyrosine kinases, in a 4-week-on, 2-week-off schedule in patients with advanced solid tumors, Clin Cancer Res, 17 (2011) 7156-7163.

[23] N. Shobeiri, M. Rashedi, F. Mosaffa, A. Zarghi, M. Ghandadi, A. Ghasemi, R. Ghodsi, Synthesis and biological evaluation of quinoline analogues of flavones as potential anticancer agents and tubulin polymerization inhibitors, European journal of medicinal chemistry, 114 (2016) 14-23.

[24] I. Khelifi, T. Naret, D. Renko, A. Hamze, G. Bernadat, J. Bignon, C. Lenoir, J. Dubois, J.D. Brion, O. Provot, M. Alami, Design, synthesis and anticancer properties of IsoCombretaQuinolines as potent tubulin assembly inhibitors, European journal of medicinal chemistry, 127 (2017) 1025-1034.

[25] A. Coluccia, D. Sabbadin, A. Brancale, Molecular modelling studies on Arylthioindoles as potent inhibitors of tubulin polymerization, European journal of medicinal chemistry, 46 (2011) 3519-3525.

[26] P.V. Sri Ramya, S. Angapelly, L. Guntuku, C. Singh Digwal, B. Nagendra Babu, V.G. Naidu, A. Kamal, Synthesis and biological evaluation of curcumin inspired indole analogues as tubulin polymerization inhibitors, European journal of medicinal chemistry, 127 (2017) 100-114.

[27] S. Aprile, E. Del Grosso, G.C. Tron, G. Grosa, In vitro metabolism study of combretastatin A-4 in rat and human liver microsomes, Drug metabolism and disposition: the biological fate of chemicals, 35 (2007) 2252-2261.

[28] J.J. Yeh, W.H. Hsu, J.J. Wang, S.T. Ho, A. Kao, Predicting Chemotherapy Response to Paclitaxel-Based Therapy in Advanced Non-Small-Cell Lung Cancer with P-Glycoprotein Expression, Respiration, 70 (2003) 32-35.

[29] G. Szakács, J.K. Paterson, J.A. Ludwig, C. Booth-Genthe, M.M. Gottesman, Targeting multidrug resistance in cancer, Nature Reviews Drug Discovery, 5 (2006) 219-234.

[30] B.C. Baguley, Multiple drug resistance mechanisms in cancer, Molecular biotechnology, 46 (2010) 308-316.

[31] M. Kavallaris, Microtubules and resistance to tubulin-binding agents, Nature reviews. Cancer, 10 (2010) 194-204.

[32] A. Ganguly, F. Cabral, New insights into mechanisms of resistance to microtubule inhibitors, Biochimica et biophysica acta, 1816 (2011) 164-171.

[33] Z. Yang, W. Wu, J. Wang, L. Liu, L. Li, J. Yang, G. Wang, D. Cao, R. Zhang, M. Tang, J. Wen, J. Zhu, W. Xiang, F. Wang, L. Ma, M. Xiang, J. You, L. Chen, Synthesis and biological evaluation of novel millepachine derivatives as a new

class of tubulin polymerization inhibitors, Journal of medicinal chemistry, 57 (2014) 7977-7989.

[34] W. Pan, Q. Wang, Y. Zhang, N. Zhang, J. Qin, W. Li, J. Wang, F. Wu, L. Cao, G. Xu, Verteporfin can Reverse the Paclitaxel Resistance Induced by YAP Over-Expression in HCT-8/T Cells without Photoactivation through Inhibiting YAP Expression, Cellular Physiology and Biochemistry, 39 (2016) 481-490.

[35] J. Zacherl, G. Hamilton, T. Thalhammer, M. Riegler, E.P. Cosentini, A. Ellinger, G. Bischof, M. Schweitzer, B. Teleky, T. Koperna, et al., Inhibition of P-glycoprotein-mediated vinblastine transport across HCT-8 intestinal carcinoma monolayers by verapamil, cyclosporine A and SDZ PSC 833 in dependence on extracellular pH, Cancer Chemother Pharmacol, 34 (1994) 125-132.

[36] F. Liu, Z.H. Xie, G.P. Cai, Y.Y. Jiang, The effect of survivin on multidrug resistance mediated by P-glycoprotein in MCF-7 and its adriamycin resistant cells, Biological & pharmaceutical bulletin, 30 (2007) 2279-2283.

[37] A. Pepe, L. Sun, I. Zanardi, X. Wu, C. Ferlini, G. Fontana, E. Bombardelli, I. Ojima, Novel C-seco-taxoids possessing high potency against paclitaxel-resistant cancer cell lines overexpressing class III β-tubulin, Bioorganic & medicinal chemistry letters, 19 (2009) 3300-3304.

[38] S. Wang, K. Fang, G. Dong, S. Chen, N. Liu, Z. Miao, J. Yao, J. Li, W. Zhang, C. Sheng, Scaffold Diversity Inspired by the Natural Product Evodiamine: Discovery of Highly Potent and Multitargeting Antitumor Agents, Journal of medicinal chemistry, 58 (2015) 6678-6696.

[39] J. Yang, S. Yang, S. Zhou, D. Lu, L. Ji, Z. Li, S. Yu, X. Meng, Synthesis, anti-cancer evaluation of benzenesulfonamide derivatives as potent tubulin-targeting agents, European journal of medicinal chemistry, 122 (2016) 488-496.

[40] S. Fortin, J. Lacroix, M.F. Cote, E. Moreau, E. Petitclerc, C.G. R, Quick and simple detection technique to assess the binding of antimicrotubule agents to the colchicine-binding site, Biological procedures online, 12 (2010) 113-117.

[41] D. Cao, X. Han, G. Wang, Z. Yang, F. Peng, L. Ma, R. Zhang, H. Ye, M. Tang, W. Wu, K. Lei, J. Wen, J. Chen, J. Qiu, X. Liang, Y. Ran, Y. Sang, M. Xiang, A. Peng, L. Chen, Synthesis and biological evaluation of novel pyranochalcone derivatives as a new class of microtubule stabilizing agents, European journal of medicinal chemistry, 62 (2013) 579-589.

[42] G. Wang, W. Wu, F. Peng, D. Cao, Z. Yang, L. Ma, N. Qiu, H. Ye, X. Han, J. Chen, J. Qiu, Y. Sang, X. Liang, Y. Ran, A. Peng, Y. Wei, L. Chen, Design, synthesis, and structure-activity relationship studies of novel millepachine derivatives as potent antiproliferative agents, European journal of medicinal chemistry, 54 (2012) 793-803.

[43] G. Wang, F. Peng, D. Cao, Z. Yang, X. Han, J. Liu, W. Wu, L. He, L. Ma, J. Chen, Y. Sang, M. Xiang, A. Peng, Y. Wei, L. Chen, Design, synthesis and biological evaluation of millepachine derivatives as a new class of tubulin polymerization inhibitors, Bioorganic & medicinal chemistry, 21 (2013) 6844-6854.

[44] G. Wang, C. Li, L. He, K. Lei, F. Wang, Y. Pu, Z. Yang, D. Cao, L. Ma, J. Chen, Y. Sang, X. Liang, M. Xiang, A. Peng, Y. Wei, L. Chen, Design, synthesis and biological evaluation of a series of pyrano chalcone derivatives containing indole moiety as novel anti-tubulin agents, Bioorganic & medicinal chemistry, 22 (2014) 2060-2079.

[45] Z. Yang, T. Wang, F. Wang, T. Niu, Z. Liu, X. Chen, C. Long, M. Tang, D. Cao, X. Wang, W. Xiang, Y. Yi, L. Ma, J. You, L. Chen, Discovery of Selective Histone Deacetylase 6 Inhibitors Using the Quinazoline as the Cap for the Treatment of Cancer, Journal of medicinal chemistry, 59 (2016) 1455-1470.

Highlights

- Twenty-six novel 4-anilinoquinoline derivatives were synthesized and evaluated for their antiproliferative activities.
- The structure-activity relationship was discussed in different ways.
- Compound **13bh** exhibited the most potent activity against all tested tumor cell lines and showed promising efficacy in multidrug resistant cancer cells.
- Compound **13bh** was identified as a novel tubulin depolymerization agent by binding at the colchicine site.
- Compound **13bh** exhibited potent inhibitory activity against tumor growth in vivo.